Journal of AI and Data Mining
Vol 8, No 4, 2020, 481-489. ***Original Research Paper*** DOI: 10.22044/JADM.2019.6985.1828

Fuzzy Adaptive Granulation Multi-Objective Multi-microgrid Energy Management

F. Sabahi*

Department of Electrical Engineering, Faculty of Engineering, Urmia University, Urmia, Iran.

Received 21 April 2018; Revised 02 March 2019; Accepted 06 August 2019
**Corresponding author: f.sabahi@urmia.ac.ir (F. Sabahi).*

Abstract
This paper develops an energy management approach for a multi-microgrid (MMG) taking into account multiple objectives involving plug-in electric vehicle (PEV), photovoltaic (PV) power, and a distribution static compensator (DSTATCOM) to improve power provision sharing. In the proposed approach, there is a pool of fuzzy microgrids granules that compete with each other to prolong their lives while monitored and evaluated by the specific fuzzy sets. In addition, based on the hourly reconfiguration of microgrids (MGs), granules learn to dispatch cost-effective resources. In order to promote an interactive service, a well-defined multi-objective approach is derived from fuzzy granulation analysis to improve power quality in MMGs. A combination of the meta-heuristic approach of genetic algorithm (GA) and particle swarm optimization (PSO) eliminates the computational difficulty of the non-linearity and uncertainty analysis of the system and improves the precision of the results. The proposed approach is successfully applied to a 69-bus MMG test with the results reported in terms of the stored energy improvement, daily voltage profile improvement, MMG operations, and cost reduction.

Keywords: *Energy Management, Multi-Microgrids, Fuzzy Logic, Plug-in Electric Vehicle (PEV), Distribution Static Compensator (DSTATCOM).*

1. Nomenclature

I) Function

ψ_6^{EV}	Charging status of a parking lot (0/1)
U_g	Utility function of a power grid
U_d	Utility function of microgrids
$\lambda(t)$	Market price at time t
V	Voltage magnitude
U_c	Constraint Function
$F_g^i(t)$	Power distribution between the power grid and the *ith* microgrid at time t
$F_d^i(t)$	Function for representing operation cost of *ith* microgrid at time t.
F_{Power}	Power supply from RES to the *ith* microgrid
C_{DG} , C_{SU} , C_{SD}	Operation startup and shut down costs of DG
$s_i(t)$	Stored energy of the *ith* microgrid at time t

II) Parameter

P_{ST} , Q_{ST}	Active and Reactive power of sub-station
P_D, Q_D	Active and Reactive power
$P_L^{i,j,n}$	Active power flow from bus n to j for microgrid
G, B	Conductance and susceptance of line
SOE_{EV}	SOE of a parking lot
η_{EV}	Efficiently of parking lot converter
$\bar{E}_{EV}$	Energy capacity of a parking lot
SOE_{arr-EV}	SOE's associated with an arrival time
SOE_{dep-EV}	SOE's associated with departure time
a	Plug status of parking lot $0/1$
$\bar{P}_{Loss}$	The upper limit for line active power losses
Ω	Coefficient indicating the priority of MG buses

V^*	Desired voltage magnitude
I	Current magnitude
$P_{W\,ind}$	Wind power generation
P_L, Q_L	Active and Reactive power consumptions of load
r_p, r_q	Wholesale electricity prices for active and reactive powers
P_{EV^+}, P_{EV^-}	Charging and discharging powers of a parking lot
Q^{DS}	DSTATCOM reactive power
P_{PV}	PVs active power transfer
η_{PV}	Power flow efficiently of PV inverter
S_{PV}	Apparent power of PV inverter
A_{PV}	PV panel surface area (m^2).
P_{in}, Q_{in}	Imported active and reactive power from a substation
C_{Tap}	Tap adjustment cost
S_{in}	Substation apparent power flow

III) Index and variable

N	The total number of Microgrids
N_s	The total number of Microgrids that have a local energy storage system
$N - N_s$	Total number of Microgrids that don't have a local energy storage system
g	DG's index
i	Index of microgrid
j	Index of microgrid's bus
t	Time index
N_B	Total number of buses
m	The number of parameters in phenotype
h	Index of individual
a	Index of generation
Tap	Tap position of ULTC.

2. Introduction

Microgrid (MG) is an alternative energy providing system that is an effective way to incorporate a high penetration of distributed resources at medium and low voltages in order to manage energy in modern industrial development. Based on the European concept of MGs, an MG can be defined as an active pattern that consists of several sources, controllable loads, and storage devices with a capacity up to a few hundreds of kilowatt (kW). MGs operate both interconnected to the main power grid and islanded.

Within a specific area, a number of nearby MGs form multi-microgrids (MMG). MMG systems have been divided into AC MMG, which are the most common, DC MMG, or AC-DC MMG based on the connection of components to AC buses, DC buses, or both [1]. An MMG configuration is shown in figure 1.

Scheduling of MMGs is a major operational challenge due to the demand response and renewable generation. However, the implementation of conventional scheduling algorithms, which are not capable of considering the stochastic nature of DERs, may lead to a mismatch in the forecast and realize the power and consequently impose extra costs to the microgrid.

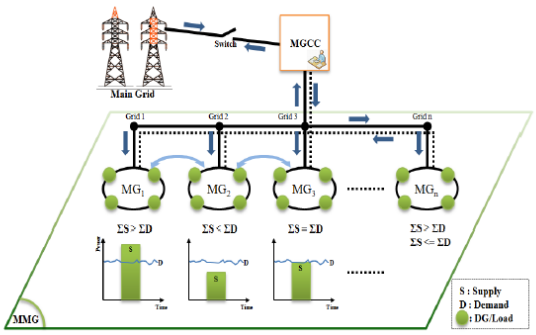

Figure 1. A Schematic representation of Multi-microgrid (a microgrid central controller (MGCC))[2].

Conventional scheduling algorithms cannot consider the stochastic nature of MG components, potentially producing errors in forecasting power, and imposing extra MG costs. For example, uncontrolled charging of PEVs at peak demands makes strict voltage drops. Power trading involves searching for the optimal amount of power to export and import within the MMG.

Meta-heuristic approaches can capture complexity and uncertainty in the process such as in weather data or load data [3]. For MG energy management, Genetic Algorithm (GA) [4] and Particle Swarm Optimization (PSO) [2, 5] are applied. In [6], a cost-benefit approach is modeled by several Decision-Aid techniques. In this approach, the analysis of robustness is done. A market mechanism integrating urgent energy transactions and contracts is introduced in [7] to improve the value of urgent energy transactions in MMG systems. In [8], a multi-objective reactive power dispatch is solved using a modified harmony search algorithm. In [9], the sequentially-coordinated operation electric energy and heat energy is introduced for optimal energy management in a cooperative MMG community. A market operator (MO) and a distribution network operator (DNO) are designed for MMG system in [10]. Using linear duality theory and Karush–Kuhn–Tucker in [11], a cost minimization deterministic model is formulated as a min-max robust counterpart for the MMG system. In [12], a multi-frequency control is proposed in the MMG system's back-to-back converter.

In this paper, we aim to provide an optimal and stable scheduling MMG design, recognizing the change points and the hidden nature of distributed

generation (DG) in the MG system. We aim to develop an approach to handle time-varying changes in the correlation structure of MGs while optimizing energy management, which is a time-ordered structure. In fact, MGs are simultaneously tracked and monitored to obtain the optimal management of energy.

The main contributions of this paper are as follow:

- *Development of an optimal approach for constructing reliable energy management considering a voltage-dependent load model.*
- *Consideration of PEV fleets as support for MMG power demands.*
- *Consideration of AC operational constraint*
- *Accounting for the non-linearity in the characteristics of the MMG components and loads characteristics without facing computational challenges*
- *Improvement of the voltage profile*
- *Integration of DSTATCOM in the proposed energy management system*
- *Consideration of both economic and power quality improvement*
- *Optimization of the utility of MGs and the power grid*
- *Flexibility stemming from the use of fuzzy granulation*

This paper's content is organized as described below. Section 3 details the proposed approach by formulating the problem. Section 4 describes and discusses the simulation results. Section 5 then states the research conclusions.

3. Proposed Approach

In this section, we first formulate MGs, followed by power grid and emergency demands, with the goal of optimizing both the economic and technical subjects.

Assumption 1: Loads are assumed available for management purposes.

Assumption 2: Power sharing is preferred between MGs rather than with power grid within MMG.

This assumption leads to the lowest price results in comparison to exchanging with the main power grid.

It should be noted that the connection/ disconnection of the microgrids to each other or to the main grid can be done using a normally open interconnecting static switch (ISS) [13] as shown in Figure 2. In this paper, we model the switching among microgrids as a local binary function illustrated by one for connecting case and zero for disconnecting.

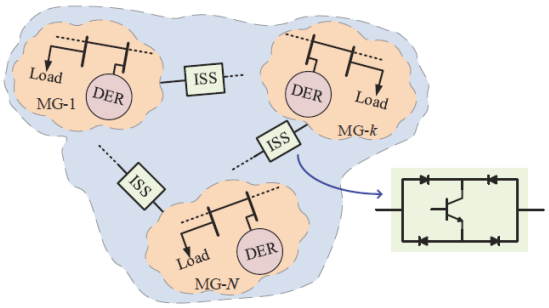

Figure 2. Connection of MGs with ISS [14].

3.1. Modeling Microgrid's Components and Constraints

The investigated MGs includes PV unit, plug-in electric vehicle (PEV), DGs, and DSTATCOM. For PEV fleets constraints [15], we calculate the state of energy (SOE) for each fleet as follows:

$$SOE_{EV}^{i,j}(t) = SOE_{EV}^{i,j}(t-1) + \frac{\eta_{EV}^{i,j}\ P_{EV+}^{i,j}(t-1)\Delta t}{\bar{E}_{EV}^{i,j}} - \frac{P_{EV-}^{i,j}(t-1)\Delta t}{\eta_{EV}^{i,j}\ \bar{E}_{EV}^{i,j}} \quad (1)$$

We assume that MG operator can undertake the charging/discharging of PEV batteries task. It should be noted that the power of all PEVs is taken into account at the aggregator level. Now, we define the model of PV, ULTC, and DSTATCOM [16].

For PV units, we calculate the power by the following:

$$P_{PV}^{i,j}(t) < \bar{P}_{PV}^{i,j} = \eta_{PV}^{i,j}\ A_{PV}^{i,j}\ I_{PV}^{i,j} \quad (2)$$

Under load tap changer (ULTC) transformer, we have:

$$(P_{in}^{i,j}(t))^2 + (Q_{in}^{i,j}(t))^2 < (\bar{S}_{in}^{i,j})^2$$
$$\underline{Tap} < Tap^{i,j}(t) \le \overline{Tap} \quad (3)$$

For *DSTATCOM*, the reactive power set-point is restricted by the following:

$$\underline{Q}_{DS}^{i,j}(t) \le Q_{DS}^{i,j}(t) \le \bar{Q}_{DS}^{i,j} \quad (4)$$

For AC power flow, constraint includes:

$$P_{ST}^{i,j}(t) + P_{DG}^{i,j}(t) + P_{Wind}^{i,j}(t) + P_{PV}^{i,j}(t) - P_{L}^{i,j}(t) - P_{D}^{i,j}(t) = \sum_{\substack{n=1 \\ n\neq j}}^{N_B} P_{L}^{i,j,n}(t) \quad (5)$$

where

$$P_{L}^{i,j,n}(t) = G^{i,j,n}(t)(V_{i,j}^2(t) - V_{i,j}(t)V_{i,n}(t)\cos(\theta_{i,j}(t) - \theta_{i,n}(t))) - B^{i,j,n}(t)(V_{i,j}(t)V_{i,n}(t)\sin(\theta_{i,j}(t) - \theta_{i,n}(t))) \quad (6)$$

and,

$$\underline{V}_{i.j} \le V_{i,j}(t) \le \overline{V}_{i.j} \tag{7}$$

$$I_{i,j}(t) \le \overline{I}_{i.j} \tag{8}$$

In addition,

$$Q_{ST}^{i.j}(t) + Q_{DG}^{i.j}(t) - Q_{L}^{i.j}(t) = \sum_{\substack{n=1 \\ n \neq j}}^{N_B} Q_{L}^{i.j,n}(t) \tag{9}$$

where

$$\begin{aligned} & Q_{L}^{i.j,n}(t) \\ & = -B^{i.j,n}(t)(V_{i,j}^{2}(t) \\ & -V_{i,j}(t)V_{i,n}(t)\cos(\theta_{i,j}(t)-\theta_{i,n}(t))) \\ & -G^{i.j,n}(t)\left(V_{i,j}(t)V_{i,n}(t)\sin(\theta_{i,j}(t)-\theta_{i,n}(t))\right) \end{aligned} \tag{10}$$

3.2. Power Grid

The total cost of microgrids is computed as follows:

$$F_{d} = \sum_{i=1}^{N} F_{d_i} \tag{11}$$

We define the assessment measure as follows:

$$a_{ss} = \frac{F_{d}^{\text{after-management}}}{F_{d}^{\text{before-management}}} \tag{12}$$

By considering $F_{g}(t) = \sum_{i=1}^{N} F_{g_i}(t)$ such as:

$$\begin{aligned} & F_{g_i}(t) > 0 \quad \text{microgrid i receives power} \\ & F_{g_i}(t) < 0 \quad \text{microgrid i sells power} \end{aligned} \tag{13}$$

We define $U_{g}\left(F_{g}(t),\lambda(t)\right)$ as the utility function of the power grid. Now, we need to maximize it:

$$\max_{F_{g_i}(t),\lambda(t)} U_{g}\left(F_{g}(t),\lambda(t)\right) \tag{14}$$

In addition, by considering $U_{d}\left(F_{d_1}(t),\ldots,F_{d_N}(t),\lambda(t)\right)$ as the utility demand function, we maximize it:

$$\max_{\lambda(t)} U_{d}\left(F_{d_1}(t),\ldots,F_{d_N}(t),\lambda(t)\right) \tag{15}$$

3.3. Emergency Demand

The emergency demand can be formulated using sorted energy $s_i(t)$, as follows:

$$\begin{aligned} & s_{i}(t+1) = s_{i}(t) + F_{g_i}(t) - F_{d_i}(t) + V_{i}(t) \\ & i \in N_{s} \end{aligned} \tag{16}$$

To describe the emergency demand, we define:

$$\max_{F_{g_i}(t),\lambda(t)} \sum_{i=1}^{N_s} s_{i}(t+1) \tag{17}$$

subject to $\underline{s}_{i} < s_{i}(t+1) < \overline{s}_{i}$

It should be noted that $\underline{s}_{i} > 0$ shows the minimum storage energy and $\overline{s}_{i}$ is the maximum stored energy.

3.4. Objective Function

The aim is to minimize the daily scheduling modeled by the following:

$$\begin{aligned} F_{d_i} &= \sum_{t}[r_{p}^{i}(t)P_{ST}^{i}(t) + r_{q}^{i}(t)Q_{ST}^{i}(t) \\ &+ \sum_{g}(C_{DG}^{i,g,t} + C_{SU}^{i,g,t} + C_{DG}^{i,g,t} \\ &+ C_{Tap}(Tap^{i.j}(t) - Tap^{i.j}(t-1)))] \end{aligned} \tag{18}$$

and

$$F_{Qulity}^{i} = \sum_{t}\sum_{j} \Omega^{i.j} \left| V_{i,j}(t) - V_{i,j}^{*} \right| \tag{19}$$

where we have $F_{g_i} - F_{d_i} + F_{Qulity}^{i} = 0$ as a constraint for $i \in N - N_{s}$. Note that the greater $\boldsymbol{\Omega}$ is the less voltage deviations are.

To address the objective functions, we formulate the proposed system as follows:

$$\max_{\lambda(t)} U_{d}\left(F_{d_1}(t),\ldots,F_{d_N}(t),\lambda(t)\right) \tag{20}$$

$$\max_{F_{g_i}(t),\lambda(t)} U_{g}\left(F_{g}(t),\lambda(t)\right) \tag{21}$$

$$\max_{F_{g_i}(t),\lambda(t)} \sum_{i=1}^{N_s} s_{i}(t+1) \tag{22}$$

subject to

$$\underline{s}_{i} < s_{i}(t+1) < \overline{s}_{i} \tag{23}$$

$$F_{g_i} - F_{d_i} + F_{Qulity}^{i} = 0 \text{ for } i \in N - N_{s} \tag{24}$$

$$\underline{V}_{i.j} \le V_{i,j}(t) \le \overline{V}_{i.j} \tag{25}$$

$$\underline{Q}_{i.j} \le Q^{DS} \le \overline{Q}_{i.j} \tag{26}$$

$$(P_{in}^{i.j}(t))^{2} + (Q_{in}^{i.j}(t))^{2} < (\overline{S}_{in}^{i.j})^{2} \tag{27}$$

Assumption 3: PEVs' charge/discharge states are assumed to be independent of solar irradiance.

3.5. Adaptive Optimization

It should be noted that an MG faces different uncertainties including those in the consumption, the distributed generation (DG) that makes deflections in energy generation and in the non-linearity existing in the real system such as wind turbine and photovoltaic coefficients, which vary with wind conditions and photo as well as uncertainty in the exact geometry of the battery. To deal with the known and unknown uncertainty, our concern is providing the ability to adapt to different situations using fuzzy logic and heuristic

approaches. Fuzzy logic helps us less dependent on the precise model as well as knowledge about the situation involved.

More specifically, the hidden nature of distributed generation that varies over time is a major problem; however, an approximate solution is helpful and can be satisfactorily applied to further development while monitoring by fuzzy membership functions. This is particularly useful during emergency demand and/or when the time is restricted.

The proposed approach aims to minimize cost and improve quality by creating a pool of fuzzy granules of MGs'structure and utilizing the results in energy management. Many process variables are tracked in this approach. The proposed approach is done online. However, to save the running time, a large space is used for the first execution of the algorithm and after that, the range of search is changed around the values obtained in the first execution. Now, we detail the proposed approach.

A random microgrids'structure population $\{M_1,\ldots,M_i,\ldots,M_N\}$ is initially created:

$$M_i=\left\{\begin{array}{c} x^a_{h,m}\,|\,x^a_{h,m}: r^i_p(t), P^i_{ST}(t), r^i_q(t), Q^i_{ST}(t),\\ V_i(t), C^{i.g,t}_{DG}, C^{i.g,t}_{SU}, C^{i.g,t}_{DG}, \Omega^{i.j}, P^{i.j}_{DG}(t),\\ P^{i.j}_{Wind}(t), P^{i.j}_{L}(t), P^{i.j}_{D}(t), Q^{i.j}_{ST}(t),\\ Q^{i.j}_{DG}(t), Q^{i.j}_{L}(t), SOE^{i.j}_{EV}(t), s_i(t) \end{array}\right\} \quad (28)$$

where $x^a_{(h,m)}$ is the h^{th} individual at the s^{th} generation and m is the number of design parameters.

The phenotype of the first chromosome $M_1=\{x^1_{1,1},\ldots,x^1_{1,r},\ldots,x^1_{1,m}\}$ is chosen as the center $C_1=\{c_{1,1},\ldots,c_{1,r},\ldots,c_{1,m}\}$. To capture changes in a continuous manner, we use Gaussian membership functions as follows $\mu_r(x^a_{h,r})=\exp(-(x^a_{h,r}-c_{1,r})^2/\sigma_r^2$ where σ is the width of the membership function. In fact, σ controls the degree of specificity of the individual; in order to have an accurate estimation of each individual σ is reduced or enlarged in reverse proportion to fitness as described below:

$$\sigma_r=\gamma\frac{1}{\left(e^{\max\left(F_{d_1}(t),\ldots,F_{d_N}(t),\lambda(t),F_g(t),\sum_{i=1}^{N_S}S_i(t+1)\right)}\right)^{\beta}} \quad (29)$$

The γ and β are problem-dependent and have to be adjusted. If one of the constraints conflicts then $\gamma=0$. To solve this nonlinear multi-objective optimization, we use a combination of genetic algorithm (GA) and particle swarm optimization (PSO).

Genetic Algorithms are most effective when the search space is little known. For solving any problem using GA, we choose a method to represent the solution of a given problem, such that we form an initial population of solutions and then evaluate each random solution based on a cost function. The cost function judges how well the random solution solves the problem. This is in the case of our problem. Therefore, here, we use GA. However, to overcome the deficiencies related to GA including the better balance between exploitation and exploration, we combine GA with the simple still applicable algorithm of PSO.

In each generation after calculating the fitness of all individuals, the population is divided into two sections; each section is evolved by one of GA or PSO algorithms. These two algorithms are recombined and then, in the next generation, randomly divided and moving on the solution space by PSO or GA. This offers a better balance between the exploitation of the search space and the exploration of unvisited search areas. The flowchart of the proposed algorithm is shown in Figure 3.

The continuous (real-coded) GA is used here. The steps of the applied GA section are as follows:

Step 1: Encoding: Each vector M is considered as an individual. There is a restriction on the range of *M* based on σ.

Step 2: Initialization: The *N* individuals, M_i's, are generated randomly.

Step 3: Fitness assignment and Evaluation: The fitness is defined. (20) and (21). The evaluation process is a little different and is divided into two cases.

Case I: When an obtained individual, constraints are not fulfilled, the fitness value is assigned small enough in order to discard this individual.

Case II: When constraints are fulfilled: The fitness is determined.

This step is repeated for the number of individuals.

Step 4: S*election:* To produce a new offspring for the next generation, two chromosomes with a roulette wheel selection method are chosen to be involved.

Step 5: Crossover: The selected individuals are recombined through the linear heuristic crossover method to guarantee that the constraints are still satisfied. The best new offsprings are propagated.

Step 6: Mutation: To make sure that GA searches the solution space freely, uniform mutation is used. The mutated gene from the search interval is

drawn randomly.

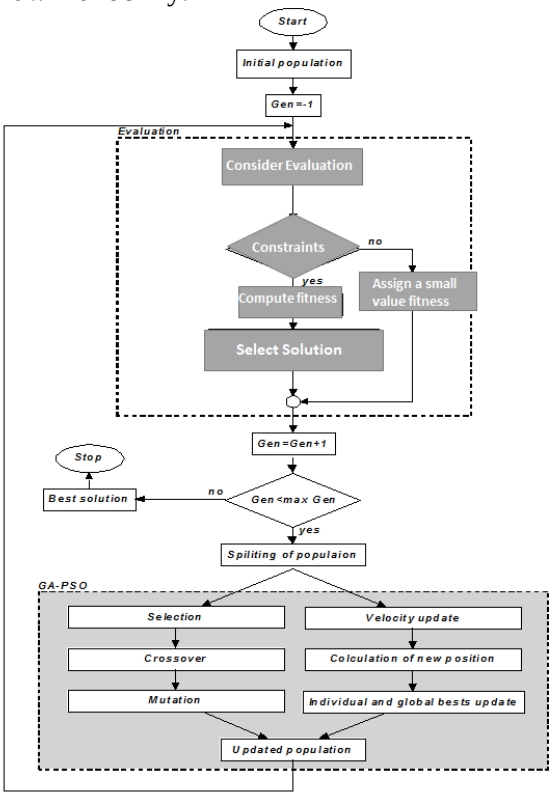

Figure 3. Flowchart of the GA-PSO algorithm.

Step 7: Elitism: The best individuals in the population are retained in the next generation.

Steps 3-7 go on until the number of generation is reached.

For the applied PSO section, it should be reminded that particle swarm optimization uses a model of social interaction to find the global optimum. The social rules are controlled by particle trajectories. At each time step, fitness function representing a quality measure is calculated by the position of each particle, as input, which represents a solution to the problem. Varying velocity explores solution space. A swarm of particles moves through the problem space with the velocity update rule that takes into account the best solution. The velocity of the particle is updated by the following rule:

$$v_i(t+1) = \varphi v_i(t) + r_1 c_1 \left(\bar{x}_{pbest} - \bar{x}_i\right) + r_2 c_2 \left(\bar{x}_{gbest} - \bar{x}_i\right) \quad (30)$$

where, $\bar{x}_{gbest}$ is the global best position and $\bar{x}_{pbest}$ is the individual best position. $\bar{x}_i, v_i$ are the position and velocity of particle *i*, respectively. Parameters r_1, r_2 are random numbers with a uniform distribution that goes from 0 to 1. Parameters c_1, c_2 are the positive acceleration constants. To prevent fluctuations around the optimal value, the term friction factor known as the initial weight has been introduced as:

$$\varphi = 1 - 0.5\frac{1-t}{1-t_{max}} \quad (31)$$

The last two terms are 'cognition (self-knowing)' and 'social knowledge' respectively. Scaling factors $\mathbf{c}_1, \mathbf{c}_2$ and $\mathbf{r}_1, \mathbf{r}_2$ are used to balance these two terms. Based on the updated velocities, each particle changes its position with the following rule:

$$x_i(t+1) = x_i(t) + v_i(t+1) F_d^i(t) F_d^i(t) \quad (32)$$

Furthermore, the combination of GA and PSO leads to a suitable hybrid method of cooperation. In the hybrid algorithm used here, a certain percent of the population in the next generation is occupied by PSO, and the remaining population is considered by the GA crossover operator [17].

4. Simulation

4.1. Test System

The proposed management approach is demonstrated through simulations with the PG and E 69-bus test distribution network. By locating three sectionalizing switches, we divide it into four microgrids. Different types of energy resources with the capacities and DSTATCOM are also added to the microgrids (Table 1). The number of AEVs is 200 vehicles that are equally divided among aggregators. When the system is working in the normal mode, these four microgrids are connected to the power grid and together. We model reactive sources as the fixed generation installed on certain buses. Figure 4 shows the locations of the sectionalizing switches and energy consumption/generation units. The price levels, for on-peak, mid-peak, and off-peak periods, are adapted from [18] (see Figure 5).

4.2. Results

Figure 6 shows the membership functions of fuzzy granules in the competitive pool before and after the update.

At first, we analyze the microgrids separately, *i.e.*, isolated mode. Figure 7 shows $F_d^i(t)$ for each microgrid with respect to the numbers of controllable units. As shown, the more controllable units the less daily costs.

Now, we consider the whole multi-microgrid system in the grid-connected mode. The total operational cost is calculated using (17-19). The 3D map of cost with respect to the number of controllable and time is shown in Figure 8. As shown, when the cost is zero or negative, it represents that energy management is selling/storing the energy within the time of using energy or buying.

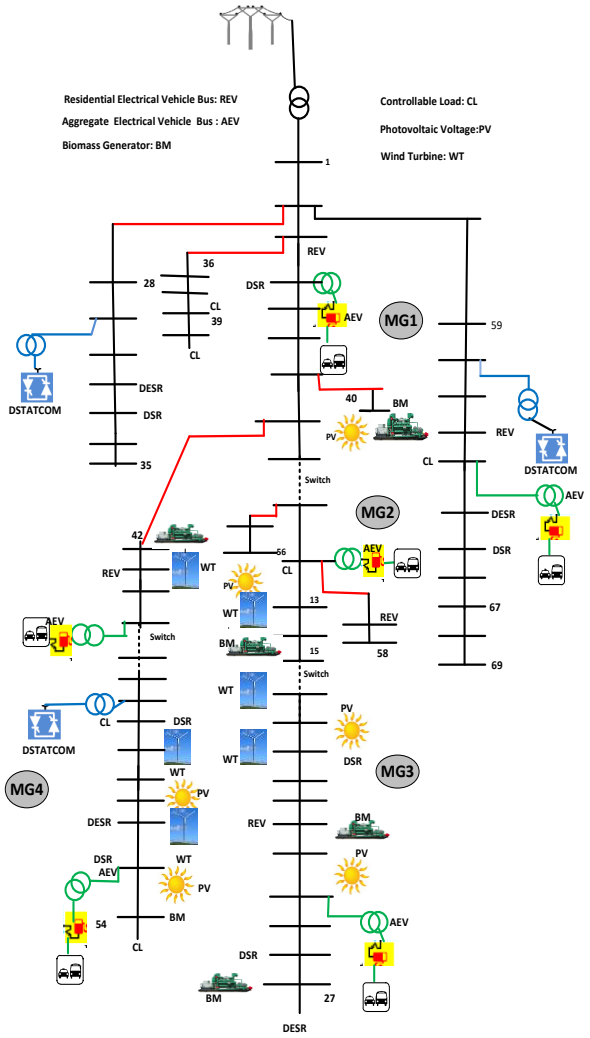

Figure 4. Schematic representation of Multi-microgrid system with its components.

Table 1. Location of energy resources.

Energy Resource	Locations (Buses)	Capacities (kW/kVAr)
Wind Turbine	13,16,19,43,49,52	50,25,50,50,50,25
PV Module	17,23,41,50,53,56	25,25,25,25,25,25
Biomass DG	15,22,27,41,42,54	100,100,100,100,100,100
Storage Units	11,27,31,48,52,64	50,50,50,50,50,50
Reactive Sources	5,19,26,33,52,65	50,50,50,50,50,50
DSTATCOM	29, 47,60	30,30.30

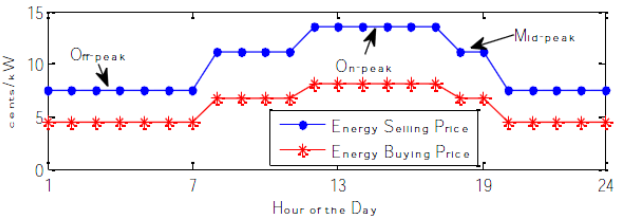

Figure 5. Hourly price of selling and buying electricity [18].

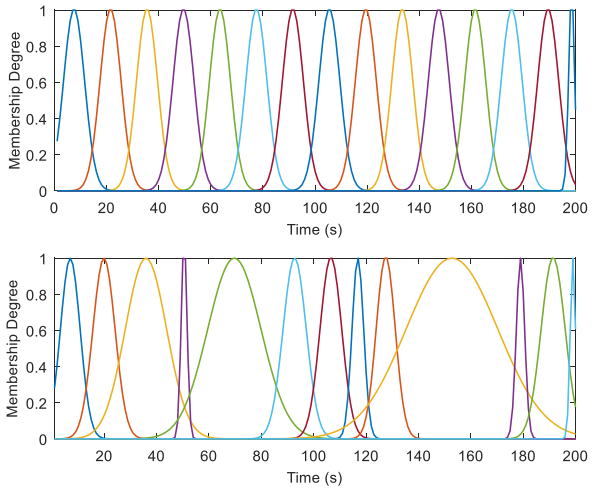

Figure 6. Fuzzy granules relevant membership functions: at first (above) and after update (below).

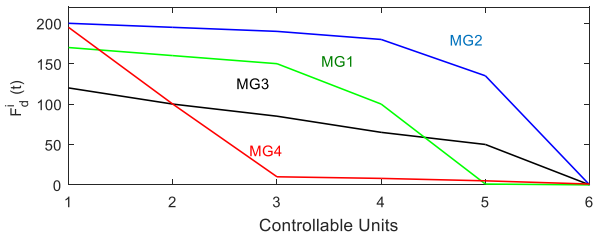

Figure 7. Variation of $F_d^i(t)$ against the number of controllable units in the isolated mode of microgrid *i*.

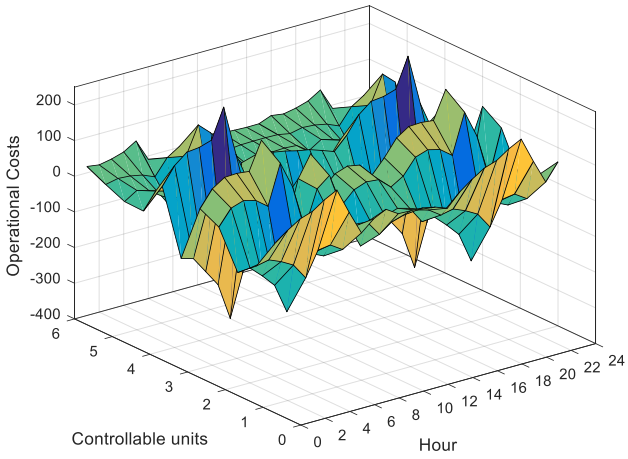

Figure 8. Variation in $F_d(t)$ verses the number of controllable units and time in grid-connected mode.

Assumption 3: At each step, one controllable unit device comes under control.

The spent calculation time for GA is calculated 29.0738 and for the proposed approach is 20.4612 for 100 runs. This shows that the proposed approach is fast in comparison.

The state of connecting/disconnecting of MG1 bandied in the network in the situation is described in Figure 9. State "0" shows the disconnection and state "1" shows the connection. In addition, the relevant energy exchange is

presented in Figure 10. As seen, when MG1 is connected to the network, in some hours, it provides energy for the network labeled by "-" and in other hours it consumes the energy labeled by "+". In hours 9-11, AM that is the peak of using energy, MG1 is disconnected, while in 14-15 P.M that is another peak of using energy, it sells energy. Table 2 shows the hours of disconnection and connection with generating/consuming the energy of the different switching of four microgrids.

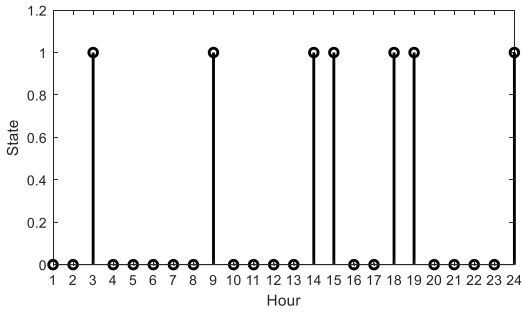

Figure 9. States of connection and disconnection of MG1.

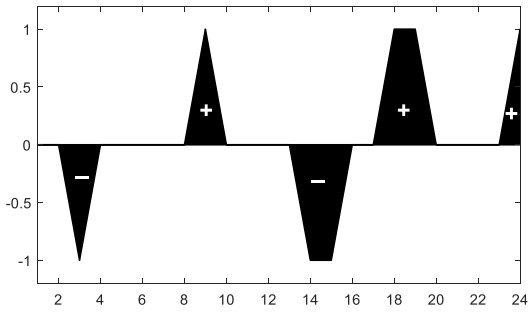

Figure 10. Energy consumption (+) and generation (-) of MG1.

Table 2. The number of connection of microgrids.

Microgrid	Connection	Generation	Consumption
MG1	7	3	4
MG2	10	6	4
MG3	7	4	3
MG4	8	3	5

The voltage profile of the multi-microgrid is depicted in Figure 11. As seen, voltage magnitude tends to 1 $p.u$ in the most of the buses. In buses 31 and 68, throughout the day, the deviation of voltage from 1 $p.u$ is more in comparison.

Figure 12 shows the aggregate EV parking lot discharges during the islanding of microgrids. Meanwhile, SOE remains at its minimum.

The reactive power contributions of buses are described in Figure 13. Some buses, especially AEV aggregators, are in capacitive operating mode. Stored energy based on the proposed management approach of four microgrids is depicted in Figure 14 versus time and the number of microgrids. It is almost in the stored mode, especially at midnight. This injected reactive power improves the voltage profile. As the figure shows, the stored energy is not negative at any of 24 hours. It reveals the effects of the proposed approach and applicability of energy management. MG1 generates sufficient power to satisfy the power shortages of other microgrids.

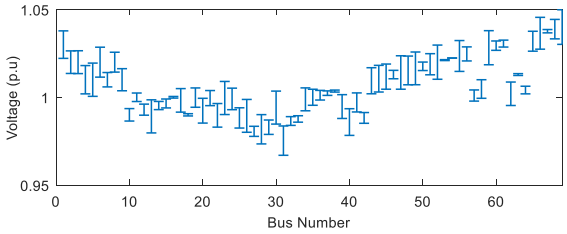

Figure 11. Daily Voltage Profile.

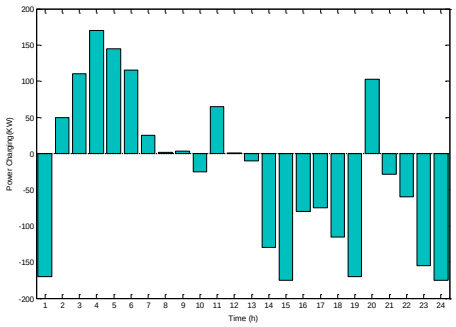

Figure 12. Charging Power of AEV.

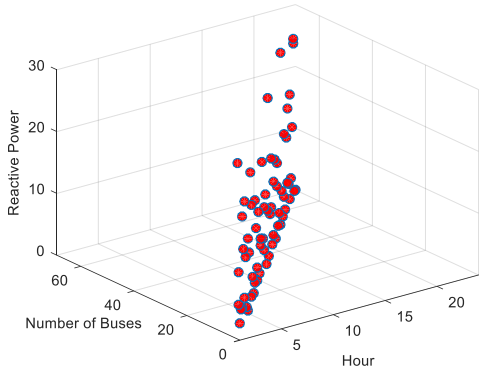

Figure 13. Reactive of Power Profile of Buses.

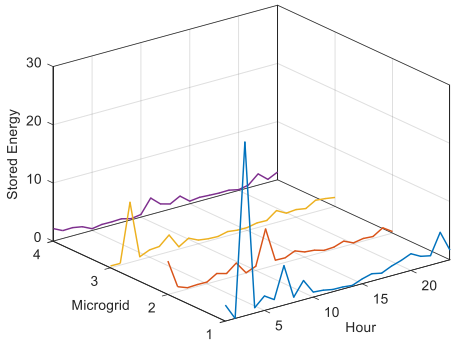

Figure 14. Stored Energy of four microgrids.

5. Conclusion

The multi-microgrid system design has been addressed in this paper. In the proposed approach, the solution is tackled through a fuzzy granulation. In order to solve the optimization problem, a fuzzy granulation GA is formulated that improves convergence speed and relationships between the independent decision variables.

Numerical studies over 69-bus are conducted which highlights the following points:

- The energy consumption issue in some hours and/or in some microgrids is resolved due to capacitive reactive power behavior.
- The dispatching pattern is improved.
- The voltage profile is increased.

It can be seen that the proposed approach is an effective tool for designing multi-microgrid in the smart network within a defined range of trade-offs.

Reference

[1] Xu, Z., Yang, P., Zheng, C., Zhang, Y., Peng, J., & Zeng, Z. (2017). Analysis on the organization and Development of multi-microgrids, Renewable and Sustainable Energy Reviews, 2017/06/30/ 2017.

[2] Pisei, S., Choi, J.-Y., Lee, W.-P., & Won, D.-J. (2017). Optimal Power Scheduling in Multi-Microgrid System Using Particle Swarm Optimization, J Electr Eng Technol, vol. 12 pp. 1329-1339, 2017.

[3] Hoke, A., Brissette, A., Chandler, S., Pratt, A. & Maksimovic, D. (2013). Look-ahead Economic Dispatch of Microgrids with Energy Storage, Using Linear Programming, in Technologies for Sustainability (SusTech), 2013 1st IEEE Conference on 2013, pp. 155-161.

[4] Chen, C., Duan, S., Cai, T., Liu, B., & Hu, G. (2011). Smart Energy Management System for Optimal Microgrid Economic Operation, IET Renewable Power Generation, vol. 5, pp. 258-267, 2011.

[5] Bae, I.-S. & Kim, J.-O. (2012). Phasor Discrete Particle Swarm Optimization Algorithm to Configure Micro-grids, Journal of Electrical Engineering and Technology, vol. 7, pp. 9-16, 2012.

[6] J. Vasiljevska, Lopes, J. A. P. & Matos, M. A. (2009). Multi-Microgrid Impact Assessment Using Multi Criteria Decision Aid Methods, in IEEE Bucharest Power Tech Conference, Romania, 2009, pp. 1-8.

[7] Farzin, H., Ghorani, R., Fotuhi-Firuzabad, M., & Moeini-Aghtaie, M. (2017). A Market Mechanism to Quantify Emergency Energy Transactions Value in a Multi-Microgrid System, IEEE Transactions on Sustainable Energy pp. 1-1, 2017.

[8] Valipour, K. & Ghasemi, A. (2017). Using a new modified harmony search algorithm to solve multi-objective reactive power dispatch in deterministic and stochastic models, Journal of AI and Data Mining, vol. 5, pp. 89-100, 2017.

[9] Song, N. O., Lee, J. H., & Kim, H. M. (2016). Optimal Electric and Heat Energy Management of Multi-Microgrids with Sequentially-Coordinated Operations, Energies, vol. 9, pp. 1-18, 2016.

[10] Chiu, W. Y., Sun, H., & Poor, H. V. (2015). A Multiobjective Approach to Multi-microgrid System Design, IEEE Transactions on Smart Grid, vol. 6, pp. 2263 - 2272 2015.

[11] Hussain, A., Bui, V. H. &, Kim, H. M. (2016). Robust Optimization-Based Scheduling of Multi-Microgrids Considering Uncertainties, Energies, vol. 9, pp. 1-21, 2016.

[12] Yoo, H. J. , Nguyen, T. T. & H. M., Kim. (2017). Multi-Frequency Control in a Stand-Alone Multi-Microgrid System Using a Back-To-Back Converter, Energies, vol. 10, pp. 1-18, 2017.

[13] Shahnia, F., Bourbour, S. & Ghosh, A., (2017). Coupling Neighboring Microgrids for Overload Management Based on Dynamic Multicriteria Decision-Making, IEEE Transactions on Smart Grid, vol. 8, pp. 969-983, 2017.

[14] Bourbour, S. & Shahnia, F. (2016). A suitable mechanism for the interconnection phase of temporary coupling of adjacent microgrids, in 2016 IEEE Innovative Smart Grid Technologies - Asia (ISGT-Asia), 2016, pp. 624-629.

[15] Shekari, T., Golshannavaz, S., & Aminifar, F. (2017). Techno-Economic Collaboration of PEV Fleets in Energy Management of Microgrids, IEEE Transactions on Power Systems, 2017.

[16] Hamidi, A., Golshannavaz, S. & Nazarpour, D. (2017). D-FACTS Cooperation in Renewable Integrated Microgrids: A Linear Multi-Objective Approach, IEEE Transactions on Sustainable Energy, 2017.

[17] Grimaldi, E. A., Gandelli, A., Grimaccia, F., Mussetta, M. & Zich, R. E. (2006). GSO: A new integrated evolutionary procedure for high dimension electromagnetic problems, in 2006 International Waveform Diversity & Design Conference, 2006, pp. 1-4.

[18] Arefifar, S. A., Ordonez. M. & Mohamed, Y. A-R I., Energy Management in Multi-Microgrid Systems—Development and Assessment, IEEE Transactions on Power Systems vol. 32, pp. 910-922 2017.

نشریه هوش مصنوعی و داده کاوی

مدیریت انرژی چند منظوره دانه‌ای انطباقی فازی برای ریزشبکه چندگانه

فرناز صباحی*

گروه برق، دانشکده فنی، دانشگاه ارومیه، ارومیه، ایران.

ارسال ۲۰۱۸/۰۴/۲۱؛ بازنگری ۲۰۱۹/۰۳/۰۲؛ پذیرش ۲۰۱۹/۰۸/۰۶

چکیده:

در این مقاله، یک رویکرد مدیریت انرژی برای ریزشبکه چندگانه (MMG) با در نظر گرفتن بخش‌های متعدد شامل وسیله نقلیه الکتریکی (PEV)، قدرت فتوولتائیک (PV)، و جبران کننده ایستا توزیع (DSTATCOM) برای بهبود تقسیم منبع انرژی پیشنهاد شده است. در این روش، مجموعه ای از دانه‌های ریز شبکه‌ی فازی وجود دارد که برای طولانی‌تر شدن حضورشان ضمن نظارت و ارزیابی توسط مجموعه‌های فازی خاص، با یکدیگر رقابت می‌کنند. علاوه بر این، بر اساس پیکربندی ساعتی ریزشبکه‌ها (MGs) ، دانه‌ها می‌توانند منابع مقرون به صرفه را داشته باشند. به منظور ارتقاء سرویس تعاملی، یک رویکرد چند هدفی خوش تعریف برمبنای تحلیل دانه‌های فازی برای بهبود کیفیت انرژی در MMG ها معرفی شده است. روش رترکیبی از رویکرد فرا اکتشافی الگوریتم ژنتیکی (GA) و بهینه‌سازی ازدحام ذرات (PSO) مشکل محاسبات غیرخطی و عدم قطعیت را از بین برده است و دقت نتایج را بهبود بخشیده است. رویکرد پیشنهادی با موفقیت در یک آزمایش به ریزشبکه چندگانه ۶۹ باسه اعمال شد و نتایج گزارش شده از نظر انرژی ذخیره شده، مشخصات ولتاژ روزانه، عملیات MMG و کاهش هزینه بهبود یافتند.

کلمات کلیدی: مدیریت انرژی، ریز شبکه‌ی جند گانه، منطق فازی، وسیله نقلیه الکتریکی (PEV)، جبران کننده ایستا توزیع (DSTATCOM).